Journal of Hazardous Materials A118 (2005) 53–65

Journal of Hazardous Materials

www.elsevier.com/locate/jhazmat

Revised estimates for continuous shoreline fumigation: a PDF approach

Muddassir Nazir, Faisal I. Khan*, Tahir Husain

Faculty of Engineering and Applied Sciences, Memorial University of Newfoundland, St. John's, Carew Building, EN 3056, NL, Canada A1B3X5

Received 13 February 2004; received in revised form 15 October 2004; accepted 16 October 2004
Available online 8 December 2004

Abstract

A probability density function (PDF) fumigation model is presented here to study the dispersion of air pollutants emitted from a tall stack on the shoreline. This work considers dispersion of the pollutants in the stable layer and within the thermal internal boundary layer (TIBL) proceeds independently. The growth of TIBL is considered parabolic with distance inland. Turbulence is taken as homogeneous and stationary. Dispersion of particles (contaminant) in lateral and vertical directions is assumed independent of each other. This assumption allows us to consider the position of particles in both directions as independent random variables. The lateral dispersion distribution within the TIBL is considered as Gaussian and independent of height. A skewed bi-Gaussian vertical velocity PDF is used to account for the physics of dispersion due to different characteristics of updrafts and downdrafts within the TIBL. We have used Weil (J.C. Weil, A diagnosis of the asymmetry in top-down and bottom-up diffusion using a Lagrangian stochastic model, J. Atmos. Sci., 47 (1990) 501–515) solutions to find out the parameters of this PDF. Incorporating finite Lagrangian integral time scale for the vertical velocity component, it is observed that it reduces the vertical dispersion in the beginning and moves the point of maximum concentration further downwind. Due to little dispersion in the beginning, there is more plume to be dispersed causing higher concentrations at large distances. The model has considered Weil and Brower's (J.C. Weil, P.R. Brower, Estimating convective boundary layer parameters for diffusion applications, Maryland Power Plant Siting Program Rep. PPSP-MP-48, Department of Natural Resources, Annapolis, MD, 1985, 37 pp.) convective limit to analyze dispersion characteristics within TIBL.

The revised model discussed here is evaluated with the data available from the Nanticoke field experiment on fumigation conducted in summer of 1978 in Ontario, Canada. The results of revised model are in good agreement with the observed data.

Keywords: Air pollution modeling; Convective boundary layer (CBL); Fumigation; Coastal area dispersion; Thermal internal boundary layer (TIBL)

1. Introduction

When wind flow from sea encounters the shoreline during the day with clear skies, the thermal effects of the ground give rise to the development of a thermal internal boundary layer (TIBL) over land surface.

The following conditions must be met for the growth of TIBL over land:

- Wind is flowing from sea to land (henceforth referred to as onshore flow).
- Land is warmer than sea.
- The air over sea is stably stratified.

The TIBL is essentially a convective boundary layer (CBL) that grows over land. Determination of the TIBL height is an important component of the coastal dispersion models since the interaction between this layer and a contaminant plume governs the location and strength of the plume's footprint. This way, the dispersion in the coastal region is significantly affected by the growth of the TIBL.

The mathematical modeling of the coastal fumigation process has considerable importance in air quality modeling. Many fumigation models have been developed for predicting ground level concentrations (GLCs) of airborne materials from tall stacks. Fumigation models presented by Lyons and Cole [17], Van Dop et al. [26], Misra [19] and Venkatram [25] are Gaussian and assume the instantaneous perfect vertical mixing of entraining plume. No provision is made in

* Corresponding author. Tel.: +1 709 737 8939; fax: +1 709 737 4042.

0304-3894/$ – see front matter © 2004 Elsevier B.V. All rights reserved.
doi:10.1016/j.jhazmat.2004.10.008

these models to account for the skewness of the vertical convective turbulence. This can lead to inaccurate predictions of concentration magnitude and its location, particularly when entrainment rate is high and the vertical plume spread at the plume–TIBL interface is small (for details see Luhar and Sawford [13]).

Luhar and Sawford [12] have used Lagrangian stochastic modeling approach to deal with the fumigation phenomenon. Normalized concentrations obtained from their model showed fair to good agreement with the results from Nanticoke field experiment and laboratory experiments of Deardorff and Willis [3]. The major problem associated with this approach is that it requires large computational time and, therefore, is often not appropriate for operational and routine calculations. To overcome this problem, Luhar and Sawford [13] introduced a fumigation model based on probability density function (PDF) of the random vertical velocity (w). They followed Misra's [19] approach in developing their model. After considering the superposition of two Gaussian distributions to approximate w probability density function, first proposed by Baerentsen and Berkowicz [1], they relaxed uniform and instantaneous mixing assumptions in Misra's [19] model. They defined values for some parameters of the bi-Gaussian PDF differently from Baerentsen and Berkowicz [1] and used simple surface reflection schemes, following Li and Briggs' [11] work. In these models the key assumption is that the displacements of source-emitted particles (contaminant) in the lateral (y) and vertical (z) directions are independent and they behave as two independent random variables at a time (t).

Luhar [15] extended Luhar and Sawford [13] PDF model by incorporating wind direction shear effects. In this work, particle positions in lateral direction (y) vary with height and, therefore, also depend on the height (z). They treated dispersion distribution in y direction (which was the function of z) separately and then superimposed it with bi-Gaussian PDF for vertical velocity (w) and established the new joint PDF. Although results of the model are in better agreement with the field observations, more statistical justification and validation are needed for their joint PDF.

In the above stated models, the Lagrangian integral time scale (T_{lz}) for vertical dispersion is considered infinite. Mason's [18] dispersion simulations using a Lagrangian model and large-eddy simulation fields show that a systematic reduction in vertical dispersion occurs with a decreasing w_*/u_* (where w_* is convective velocity and u_* is friction velocity) and increasing wind speed. This encourages the use of the finite vertical Lagrangian integral time scale (T_{lz}) for modeling the physics of dispersion within the TIBL.

In the present work, authors have incorporated the finite Lagrangian integral timescale for vertical dispersion to develop revised fumigation model utilizing the work of Weil et al. [31]. Authors have assumed the Gaussian distribution in lateral direction within the TIBL. The skewness in the vertical direction is accounted for using bi-Gaussian PDF for w. The growth of the TIBL is considered as parabolic for stable onshore flows following the work of Garratt [7]. Further, we neglect stream-wise diffusion (i.e., $U/w_* > 1.2$) and consider strong convection within the TIBL. In the present model, we used Weil and Brower's [27] convective limit to find various characteristics of vertical velocity in the TIBL. The details of the TIBL and the revised model are presented in subsequent sections.

2. The thermal internal boundary layer

Modeling of the TIBL height is a vital component of the fumigation phenomenon. The interaction between the TIBL and a plume influences the distribution of GLCs. We have considered Garratt's [7] 'zero order jump' or slab model for the growth of the TIBL.

$$z_i(x) = \left(\frac{2(1+2\beta)Hx}{\rho c_p \gamma U}\right)^{1/2} \tag{2.1}$$

where x is the downwind or inland distance from the land–water interface, U is mean wind speed (independent of height), H is overland heat flux, c_p is specific heat at constant pressure, γ is lapse rate for upwind condition or above the boundary layer and β is ratio of the downward heat flux at the TIBL to the upward heat flux at the surface; its value is approximately 0.2 for the CBL over land.

The above model is also used in CALPUFF; a US Environmental Protection Agency (USEPA) regulatory model. In more general form:

$$z_i(x) = A_0 x^{1/2} \tag{2.2}$$

where A_0 is the function of above stated parameters (e.g., U, H, γ, β and c_p) and is defined as:

$$A_0 = \left(\frac{2(1+2\beta)H}{\rho c_p \gamma U}\right)^{1/2} \tag{2.3}$$

where A_0 is used as an input parameter to determine the plume–TIBL interface location.

Analytical parameterizations of the TIBL height based on the slab approach are widely used in coastal dispersion models. However, they tend to have singular behavior when the stability of the onshore flow is close to neutral. Luhar [14] has derived a new analytical model, which is valid for neutral onshore flow conditions, as well. In the present work, we focus on stable onshore flow condition, which is analogous to that observed during Nanticoke fumigation experimental study. Therefore, the use of slab model for the present purpose is justified. However, we have incorporated a minor revision in the model. For instance, far distance downwind TIBL attains its full depth and the above stated Eq. (2.2) for parabolic growth does not work. In that situation equilibrium height z_{eq} can be given as:

$$z_{eq} = w_* t_* \tag{2.4}$$

where w_* is the convective velocity scale and is given by the following expression:

$$w_* = \left[\frac{gH}{\rho c_p T_s} z_{\text{eq}}\right]^{1/3} \tag{2.5}$$

and T_s is the ground surface temperature.

Considering the expression for w_*, as given by Eq. (2.5), and after some rearrangements z_{eq} can be presented as:

$$z_{\text{eq}} = \left[\left(\frac{gH}{\rho c_p T_s}\right)^{1/3} t_*\right]^{3/2} \tag{2.6}$$

where t_* is the convective time scale and we adopt its empirical value of 10 min as suggested by Stull [22]. Subsequently, using the Eq. (2.2), the horizontal distance corresponding to equilibrium height can be determined.

The non-dimensional entrainment rate at the point of interception of the plume-centerline and the TIBL, (similar to Luhar and Sawford [13]), is expressed as:

$$\frac{w_{\text{eo}}}{w_*} = 0.5 \frac{UA_0^2}{w_* z_{i0}} \tag{2.7}$$

The convective velocity w_* (corresponding to the point of interception of the plume-centerline and the TIBL) is considered to be invariant with downwind distance, as an increase in the TIBL height with downwind distance is balanced by the decrease in heat flux. Their product, which seems to cause the change in w_*, does not vary strongly with downwind distance (Venkatram [23], Misra [19]). Subsequently, we have also observed that variation of w_* with x makes insignificant difference in dispersion calculations when compared to those with a constant w_*.

3. The PDF model

A probability density function model, to calculate the concentration profiles of pollutants from an elevated continuous point source within the convective boundary layer, is derived first. Later, the fumigation model to estimate continuous shoreline fumigation is developed considering the mean structure of the TIBL, analogous to mixed layer within the CBL.

3.1. PDF model for an elevated continuous point source within convective boundary layer

A simple calculation of the ensemble-mean concentration distribution, $C(x, y, z)$, follows from mass flux considerations. The mean horizontal flux without considering the stream wise dispersion of particles through an elemental area $\Delta y \Delta z$ normal to the mean wind (U) is $UC(x, y, z)\Delta y \Delta z$ (see Fig. 1). This equals the emission rate Q times the probability of particles $p_{yz}(y, z; x/U)\Delta y \Delta z$ in the intervals $(y - \Delta y/2) < y < (y + \Delta y/2)$ and $(z - \Delta z/2) < z < (z + \Delta z/2)$. It can be prescribed as:

$$UC(x, y, z)\Delta y \Delta z = Q p_{yz}\left[y, z; \frac{x}{U}\right]\Delta y \Delta z \tag{3.1}$$

$$C(x, y, z) = \frac{Q}{U} p_{yz}\left(y, z; \frac{x}{U}\right) \tag{3.2}$$

In the above equations it is assumed that transport by bulk motion due to mean wind in the x direction (considered as the direction of wind) exceeds the stream-wise effective diffusion. It is commonly assumed that this condition is met for CBL when $U/w_* > 1.2$. In Eq. (3.2), $p_{yz}(y, z; x/U)$ is the joint density of particle position in y and z at time t (where t is x/U). Turbulence is idealized as homogeneous and stationary. The mean wind speed (U) is assumed to be uniform with height and it does not change direction with height. The lateral and vertical velocity fluctuations are assumed to be statistically independent. As a result, the displacements of source-emitted particles in the lateral (y) and vertical (z) directions are independent and they behave as two independent random variables, at a time t. Therefore,

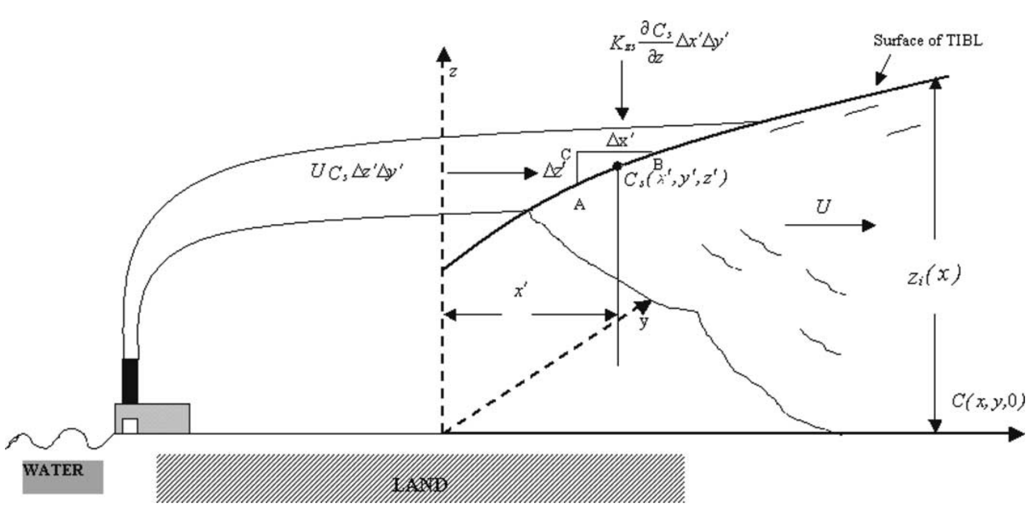

Fig. 1. Schematic of shoreline fumigation and geometry used to derive the expression for the ground-level concentration during fumigation.

$$p_{yz}\left(y, z; \frac{x}{U}\right) = p_y\left(y; \frac{x}{U}\right) p_z\left(z; \frac{x}{U}\right) \tag{3.3}$$

For convenience, the source is considered at origin having the coordinates in the horizontal plane of (0, 0). In the above density function it is assumed that the particle is released at the source height (z_s) at $t = 0$.

From Eqs. (3.2) and (3.3)

$$C(x, y, z) = \frac{Q}{U}\left[p_y\left(y; \frac{x}{U}\right) p_z\left(z; \frac{x}{U}\right)\right] \tag{3.4}$$

and $p_y(y; x/U)$ and $p_z(z; x/U)$ are normalized so that their integrals over all y and z equal one.

In Eq. (3.4) if the density functions for $p_y(y; x/U)$ and $p_z(z; x/U)$ are assumed as Gaussian then the plume model will be Gaussian. But due to the skewness of vertical velocities, a Gaussian plume model does not work well in describing the dispersion features in the CBL. Now the task is to find the appropriate $p_y(y; x/U)$ and $p_z(z; x/U)$, which can model the dispersion characteristics more realistically. Weil [29] and Weil et al. [31] have considered $p_y(y; x/U)$ being Gaussian while $p_z(z; x/U)$ is derived from the skewed w PDF, $p_w[w(z)]$, first proposed by Baerentsen and Berkowicz [1]. Weil [29] and Weil et al. [31] have related $p_z(z; x/U)$ of the particle height (z) with $p_w[w(z)]$ as:

$$p_z = p_w[w(z)]\left|\frac{\mathrm{d}w}{\mathrm{d}z}\right| \tag{3.5}$$

where the particle height (z) is a monotonic function of w. The relationship between w and z is found from a differential equation governing the particle trajectory:

$$w(z) = \frac{\mathrm{d}z}{\mathrm{d}t} \tag{3.6}$$

If w is independent of height, the differential equation is simply integrated to yield:

$$z = z_s + wt \tag{3.7}$$

where $t = x/U$ and z_s is the source height. Hence

$$z = z_s + \frac{wx}{U}. \tag{3.8}$$

In the above integration it is assumed that vertical Lagrangian integral time scale (T_{lz}) is infinitely long, so that the particle velocity at any x (downwind distance) is uniquely determined by its value at the source. So from Eq. (3.8):

$$w = (z - z_s)\frac{U}{x} \tag{3.9}$$

This is an approximation that is partially justified by the large time scales ($z_i/w_* \sim 10$ min) of the CBL convection elements. In the case of finite T_{lz} the solution of the differential Eq. (3.6) must account for the short and long-time limits of Taylor's dispersion theory. Then the obvious solution of Eq. (3.6) may be given as:

$$z = z_s + \frac{wx}{f_{lz}U} \tag{3.10}$$

where

$$f_{lz} = \left(1 + 0.5\frac{x}{UT_{lz}}\right)^{1/2} \tag{3.11}$$

$$T_{lz} = \int_0^{t\to\infty} R_w(\tau)\mathrm{d}\tau = \frac{0.7z_i w_*}{w_*} \tag{3.12}$$

In the above equation, $R_w(\tau)$ is autocorrelation function for vertical velocity (w); and since the turbulence is stationary, it is the function of the time lag (τ) between the particle velocity at ($t + \tau$) and at time (t). We adopt the parameterization for T_{lz} as $0.7z_i/w_*$ after Weil et al. [31]. Here z_i is the boundary layer height.

The convenient function f_{lz} in the trajectory Eq. (3.10) satisfies both the short and long-time limits of finite T_{lz}. After rearranging Eq. (3.10), expression for w may be given as:

$$w = (z - z_s)\frac{Uf_{lz}}{x} \tag{3.13}$$

$$\frac{\mathrm{d}w}{\mathrm{d}z} = \frac{Uf_{lz}}{x} \tag{3.14}$$

Now from Eqs. (3.5) and (3.14), the expression of p_z is given by:

$$p_z = p_w[w(z)]\frac{Uf_{lz}}{x} \tag{3.15}$$

Considering the lateral dispersion as Gaussian, the probability density function of the particle position in the lateral direction p_y is:

$$p_y = \frac{1}{\sqrt{2\pi}\sigma_{yt}}\exp\left[-\frac{y^2}{2\sigma_{yt}^2}\right]. \tag{3.16}$$

Putting the expressions for p_z and p_y from Eqs. (3.15) and (3.16) into Eq. (3.4) the following expression for a continuous elevated point source within the CBL is obtained:

$$C(x, y, z) = \frac{Q}{(2\pi)^{1/2}\sigma_{yt}x}\exp\left(-\frac{y^2}{2\sigma_{yt}^2}\right) p_w^{\Sigma} f_{lz} \tag{3.17}$$

To include reflections at the boundaries, the w PDF must be summed up over all w values that yield significant p_w values. Henceforth, the w PDF including reflection treatment from boundaries will be represented as p_w^{Σ} and its detailed description is presented in Section 3.3.1.

3.2. PDF model for an elevated continuous point source located on shoreline

A tall stack situated at the shoreline emits pollutants into the stable layer. The plume travels with relatively little dispersion in this layer and intersects the TIBL at some distance downwind resulting into fumigation. It leads to high ground level concentrations. As discussed in Misra [19], the dispersion of the pollutants in the stable layer and within the TIBL is considered to proceed independently. Now for the dispersion characteristics within the TIBL, the source strength is provided by the concentration field within the stable layer and the growth of the TIBL with distance inland. Misra [19] assumed an elevated area source coincident with the under surface of the top of the TIBL, for the dispersion of pollutants within the TIBL. The same approach is followed by Venkatram [25], Luhar and Sawford [13] and Luhar [15]. In the present model, the same source strength of pollutants for the dispersion in the TIBL is assumed.

The flux $F(x', y', z')$, from the concentration field in the stable layer to the TIBL through an infinitesimal arc AB is the sum of downward flux through CB and advective flux through AC (as shown in Fig. 1). The source strength associated with the infinitesimal arc AB can be written mathematically as:

$$dQ(x', y', z') = K_{zs}\frac{\partial C_s}{\partial z}\Delta x'\Delta y' + UC_s\Delta z'\Delta y' \qquad (3.18)$$

where $z' = z_i(x')$ and $\Delta z' = \frac{dz_i(x')}{dx}\Delta x'$

Eq. (3.18) may take the form:

$$dQ(x', y', z') = \left(K_{zs}\frac{\partial C_s}{\partial z} + UC_s\frac{dz_i(x')}{dx}\right)\Delta x'\Delta y' \qquad (3.19)$$

where K_{zs} is the diffusivity coefficient in the stable layer and is given as:

$$K_{zs} = \frac{1}{2}\frac{d\sigma_{zf}^2}{dt} \qquad (3.20)$$

In the stable layer, the distributions of velocities in both the horizontal and vertical directions are expected to be well represented by a Gaussian distribution, so do the concentrations:

$$C_s(x', y', z; H) = \frac{Q}{2\pi U\sigma_{yf}\sigma_{zf}}\exp\left[-\frac{(z-H)^2}{2\sigma_{zf}^2} - \frac{y'^2}{2\sigma_{yf}^2}\right] \qquad (3.21)$$

It is assumed that material entrained in the TIBL cannot affect the concentration in the stable layer, so no reflection term is included in Eq. (3.21).

Using Eqs. (3.20) and (3.21), the elemental source strength can be given as:

$$dQ = C_s U\left[\frac{dz_i(x')}{dx'} - \frac{d\sigma_{zf}}{dx'}\frac{(z_i(x') - H(x'))}{\sigma_{zf}}\right]\Delta x'\Delta y' \qquad (3.22)$$

If the joint PDF for the particle position in the lateral and vertical directions at time t, within the TIBL, is designated as $p_{yz}(y, y', z, z_i(x'); (x-x')/U)$ then the concentration $dC(x, y, z < z_i|x', y', z_i(x'))$ associated with $dQ(x', y', z_i(x'))$ (similar to Eq. (3.2)) can be given as:

$$dC(x, y, z < z_i|x', y', z_i(x')) = \frac{dQ}{U}\left[p_{yz}\left(y, y', z, z_i(x'); \frac{x-x'}{U}\right)\right] \qquad (3.23)$$

For the same reasons as discussed earlier, the joint PDF will take the form:

$$p_{yz}\left(y, y', z, z_i(x'); \frac{x-x'}{U}\right) = p_y\left(y, y'; \frac{x-x'}{U}\right)p_z\left(z, z_i(x'); \frac{x-x'}{U}\right) \qquad (3.24)$$

Here the shape of PDF p_y is assumed Gaussian, that is:

$$p_y\left(y, y'; \frac{x-x'}{U}\right) = \frac{1}{\sqrt{2\pi}\sigma_{yt}}\exp\left(-\frac{(y-y')^2}{2\sigma_{yt}^2}\right) \qquad (3.25)$$

The form of $p_z(z, z_i(x');(x-x')/U)$ is derived from the w PDF, which is skewed and results in a non-Gaussian p_z. The relationship between the PDF of vertical position z of a particle (p_z) and the PDF of vertical velocity (p_w^{Σ}) is already explained and can be presented as:

$$p_z\left(z, z_i(x'); \frac{x-x'}{U}\right) = p_w^{\Sigma}\frac{Uf_{lz}}{x-x'} \qquad (3.26)$$

Using Eqs. (3.24)–(3.26), Eq. (3.23) turns out to be:

$$dC(x, y, z < z_i|x', y', z_i(x')) = \frac{dQf_{lz}}{\sqrt{2\pi}(x-x')\sigma_{yt}}\exp\left(-\frac{(y-y')^2}{2\sigma_{yt}^2}\right)p_w^{\Sigma} \qquad (3.27)$$

where σ_{yt} is the crosswind spread or standard deviation within the TIBL.

Now the total concentration $C(x, y, z<z_i(x))$ due to all such sources located anywhere between 0 and x along the mean wind direction and $-\infty$ to $+\infty$ in the lateral direction is obtained by:

$$C(x, y, z < z_i(x)) = \int dC(x, y, z < z_i|x', y', z_i(x')) \qquad (3.28)$$

After relaxing the uniform and instantaneous mixing assumption of Misra [19] and Venkatram [25] and by making the provision of variation of the plume height in the region above the TIBL prior to fumigation, the final expression is:

$$C(x, y, z < z_i(x)) = \frac{Q}{2\pi}\int_0^x \frac{f_{lz}(x, x')G(x')}{(x-x')\sigma'} \times \exp\left[-\frac{p^2}{2} - \frac{y^2}{2\sigma'^2}\right]p_w^{\Sigma}dx' \qquad (3.29)$$

where

$$p(x') = \frac{z_i(x') - H(x')}{\sigma_{zf}(x')} \qquad (3.30)$$

$$G(x') = \frac{1}{\sigma_{zf}}\left[\frac{dz_i(x')}{dx'} - p\frac{d\sigma_{zf}(x')}{dx'}\right] = \frac{dp(x')}{dx'} + \frac{1}{\sigma_{zf}}\frac{dH(x')}{dx'} \qquad (3.31)$$

$$\sigma'^2(x') = \sigma_{yf}^2(x') + \sigma_{yt}^2(x-x') \qquad (3.32)$$

$H(x')$ is the plume effective height in the region above the TIBL and σ_{yf} and σ_{zf} are the dispersion spreads due to plume buoyancy in the lateral and vertical directions in the same region. Also, $z_i(x)$ is the TIBL height at distance where $x > x'$, σ_{yt} is the lateral dispersion spread due to the TIBL turbulence. Elemental sources are located at $z_i(x')$ at the plume–TIBL interface.

The present model is similar to that presented by Luhar and Sawford [13] with addition of the term f_{lz}, which accounts for the effect of finite Lagrangian integral time scale for vertical velocities. Further, we use the Weil [30] approach to parameterize the six unknown parameters of p_w^{Σ}, which is discussed in the Section 3.3.1.

3.3. PDF model parameters and their significance

3.3.1. The PDF of the vertical velocity

According to Li and Briggs [11], the form assumed for w PDF is the most important parameter for dispersion modeling in the CBL. Baerentsen and Berkowicz [1] were the first who superimposed the Gaussian distributions of vertical velocities in updrafts and downdrafts to characterize the skewed PDF of the vertical velocity component w. Many other researchers have used the same PDF for dispersion modeling in CBL (e.g., Luhar and Sawford [13], Weil [29,30] and Weil et al. [31]).

The generalized form of this w PDF is given as:

$$p_w = \frac{\lambda_1}{\sqrt{2\pi}\sigma_{w1}} \exp\left[-\frac{(w-\overline{w}_1)^2}{2\sigma_{w1}^2}\right] + \frac{\lambda_2}{\sqrt{2\pi}\sigma_{w2}} \exp\left[-\frac{(w-\overline{w}_2)^2}{2\sigma_{w2}^2}\right] \tag{3.33}$$

where λ_1 and λ_2 are weighting coefficients for the updraft and downdraft distributions, respectively, and their sum is 1. The $\overline{w}_j$ and σ_{wj} ($j = 1, 2$) are the mean vertical velocity and standard deviation for each distribution and are assumed to be proportional to the overall root mean square vertical turbulence velocity (σ_w). The six parameters λ_1, λ_2, $\overline{w}$, $\overline{w}$, σ_{w1} and σ_{w2} used in the w PDF are functions of σ_w, the vertical velocity skewness ($S = \overline{w}^3/\sigma_w^3$) and a parameter $R = \sigma_{w1}/\overline{w}_1 = -\sigma_{w2}/\overline{w}_2$ (Weil et al. [30]). From the laboratory data analysis Weil et al. [31] reported that $R = 1$ yields fair to good agreement between the modeled and measured crosswind-integrated concentration under strong convection. In the upper 90% of the CBL, the vertical velocity variance σ_w^2 can be considered to be uniform (Weil et al. [31]), as is the skewness (Wyngaard [32]). The expression for σ_w can be written as (Weil et al. [31]):

$$\sigma_w^2 = 1.2u_*^2 + 0.31w_*^2 \tag{3.34}$$

where the value 1.2 corresponds to Hicks' [8] neutral limit ($w_* = 0$) and the value 0.31 is consistent with Weil and Brower's [27] convective limit ($u_* = 0$). Hence $\sigma_w/w_* = 0.56$ from Eq. (3.34) during the strong convective regime. In the convective limit S is suggested as 0.6, which is the vertically averaged value from the Minnesota experiments (Wyngaard [32]).

By using the above values for R, S and σ_w/w_*, the values for λ_1 and λ_2 turn out as 0.4 and 0.6, respectively. Luhar [15] also parameterized the same values for λ_1 and λ_2. In another study of the bi-Gaussian PDF, Du et al. [6] specified $\lambda_1 = 0.4$ and $\lambda_2 = 0.6$ for strong convection.

The other parameters are characterized as $\overline{w}_1 = 0.488w_*$, $\overline{w}_2 = -0.32w_*$, $\sigma_{w_1} = \overline{w}_1$ and $\sigma_{w_2} = |\overline{w}_2|$. The first four parameters (i.e. λ_1, λ_2, $\overline{w}_1$, $\overline{w}_2$) are obtained by utilizing the zeroth through third moments and the last two parameters (i.e. σ_{w_1}, σ_{w_2}) are parameterized in terms of average vertical velocities in updrafts and downdrafts, respectively (Weil [30] and Weil et al. [31]). From these parameterizations it is evident that mean velocity of updrafts is larger then those of downdrafts.

To include reflections at the boundaries, the w PDF should be summed over all w values that yield significant PDF values. We have revised the simple reflection scheme of Li and Briggs [11] to include the finite T_{lz} effect within the TIBL, which takes the form:

$$w = (\pm z - z_s + 2Nz_i)\frac{Uf_{lz}}{(x-x')} \tag{3.35}$$

In this simple reflection scheme (after Luhar and Sawford [13] and Luhar [15]), $z_s = z_i(x')$ and $z_i = z_i(x)$ are assumed, thus, Eq. (3.35) transforms to:

$$w = (\pm z - z_i(x') + 2Nz_i(x))\frac{Uf_{lz}}{(x-x')} \tag{3.36}$$

where N is any integer, and $|N|$ is the number of times reflection from z_i occurs. For calculating the ground level concentration (GLC), i.e., $\pm z = 0$, the term $+z = 0$ and $-z = 0$ should be used to calculate w in the above expression. The direct trajectory is represented by $N = 0$. A value of parameter $|N|$ up to 4 is significant for the GLC calculations at distance far downwind from the source.

Finally, the vertical velocity (w) PDF in the summation form is given as:

$$p_w^{\Sigma} = \sum_{k=-N}^{N}\sum_{j=1}^{2}\frac{\lambda_j}{\sqrt{2\pi}\sigma_{wj}}\left[\exp\left[-\frac{(w_1-\overline{w}_j)^2}{2\sigma_{wj}^2}\right] + \exp\left[-\frac{(w_2-\overline{w}_j)^2}{2\sigma_{wj}^2}\right]\right] \tag{3.37}$$

where

$$w_1 = (+z - z_i(x') + 2kz_i(x))\frac{Uf_{lz}}{(x-x')} \tag{3.38}$$

$$w_2 = (-z - zi(x') + 2kzi(x))\frac{Uf_{lz}}{(x-x')} \tag{3.39}$$

3.3.2. Expressions for plume rise and vertical and lateral dispersion coefficients in stable layer

The plume's internal turbulence buoyancy controls the dispersion in onshore stable flows of plumes from tall stacks, prior to fumigation (e.g., Briggs [2] and Luhar et al. [16]).

Final rise of a buoyant plume dispersing in a stably stratified environment according to Briggs' [2] expression is:

$$z'_{\mathrm{eq}} = 2.6\left[\frac{F_0}{(UN_{\mathrm{e}}^2)}\right]^{1/3} \tag{3.40}$$

where N_{e} is natural frequency in the stable boundary layer (SBL), known as Brunt–Vaisala frequency and is given as:

$$N_{\mathrm{e}} = \left[\frac{g\gamma}{T_{\mathrm{a}}}\right]^{1/2} \tag{3.41}$$

where γ is the change of potential temperature with height (K/m), T_{a} is the ambient temperature (K), F_0 is the buoyancy flux ($\mathrm{m}^4/\mathrm{S}^3$) given by

$$F_0 = \frac{g v_{\mathrm{s}} D_{\mathrm{s}}^2 (T_{\mathrm{gs}} - T_{\mathrm{a}})}{4T_{\mathrm{a}}},$$

T_{gs} is the gas temperature at stack exit (K) and D_{s} is the inside diameter of the stack exit (m). As long as the buoyant plume has a temperature excess over the surrounding atmosphere, the plume will continue to rise. For buoyant plumes, this transitional plume rise is estimated as (Briggs [2]):

$$z'_n = 1.6F_0^{1/3}x^{2/3}U^{-1} \tag{3.42}$$

Comparing Eqs. (3.40) and (3.42), the distance where final plume rise is achieved can be determined as:

$$x_f = 2.07UN_{\mathrm{e}}^{-1} \tag{3.43}$$

So the plume rise Δh can be defined at some downwind distance as $z_n{}'$ for $z_n{}' < z_{\mathrm{eq}}{}'$ and $z_{\mathrm{eq}}{}'$ otherwise. If the distance where the lower portion of the plume intersects the TIBL is greater than x_f then Misra's (1980) parameterization for the term $G(x')$ is used in the present model equation, i.e., the term $\mathrm{d}H(x)/\mathrm{d}x'$ becomes zero in Eq. (3.31). Otherwise in the case where the buoyant plume in the region above the TIBL changes height prior to fumigation, the formulation given in Eq. (3.31) will be considered.

When the plume's internal turbulence generated by buoyancy, dominates plume dispersion in a non-turbulent environment then according to Briggs [2], plume radius grows as:

$$r = \beta_1 z'_n \tag{3.44}$$

where β_1 (0.4–0.6) is an entrainment parameter.

Luhar and Young [16] assumed the spread of the plume as:

$$\frac{r}{\sqrt{2}} = 0.35z'_n \tag{3.45}$$

Considering Eq. (3.45) coupled with the influence of the stable stratification, after Luhar and Young [16], the vertical dispersion parameter σ_{zf} can be expressed as:

$$\sigma_{zf} = 0.35\Delta h \tag{3.46}$$

The lateral dispersion coefficient, which is not influenced by the stable stratification, is given as:

$$\sigma_{yf} = 0.35z'_n \tag{3.47}$$

3.3.3. *Expression for lateral dispersion coefficient within TIBL*

The lateral dispersion in the TIBL is assumed to be dominated by ambient turbulence. This lateral spread is parameterized as (e.g., Venkatram [25], Weil [29] and Luhar and Young [16]):

$$\sigma_{yt} = \sigma_v t\left(1 + \frac{0.5t}{T_{\mathrm{ly}}}\right)^{-1/2} \tag{3.48}$$

Weil et al. [31] presented the following expression for the lateral velocity variance:

$$\sigma_v^2 = 3.6u_*^2 + 0.31w_*^2 \tag{3.49}$$

Although Draxler [4] suggested a value of 500 for T_{ly}, in the present work its value is adopted as $T_{\mathrm{ly}} = 0.7z_i/w_*$ following Weil and Corio [28]. From the above discussion and also considering Weil and Brower's [27] convective limit ($u_* = 0$), Eq. (3.48) takes the form in the present model as:

$$\sigma_{yt}(x, x') = \frac{0.56w_*(x - x')}{Uf_{\mathrm{ly}}} \tag{3.50}$$

where

$$f_{\mathrm{ly}}(x, x') = \left[1 + \frac{0.5(x - x')}{UT_{\mathrm{ly}}}\right]^{1/2} \tag{3.51}$$

This function satisfies the short and long time limits of statistical theory and takes care of the finite lateral Lagrangian integral time scale.

3.3.4. *Vertical dispersion within TIBL*

Within the TIBL, dispersion of particles occurs in updrafts and downdrafts. The distribution characteristics and strength of updrafts and downdrafts in the CBL are different. Lamb [10] reported that turbulent energy in updrafts is higher than in downdrafts. It is also understood that the mean velocity of updrafts is larger than downdrafts. So vertical dispersion of plume particles depend on their presence in updrafts or downdrafts. If it is considered that vertical Lagrangian time scale is infinite then vertical dispersion is given by:

$$\sigma_{zj}(x, x') = \sigma_{wj}\frac{x - x'}{U} \tag{3.52}$$

where $j = 1, 2$ represents the updraft and downdraft, respectively. After taking the finite Lagrangian integral time scale into account, vertical dispersion term becomes:

$$\sigma_{zj}(x, x') = \sigma_{wj}\frac{x - x'}{Uf_{\mathrm{lz}}} \tag{3.53}$$

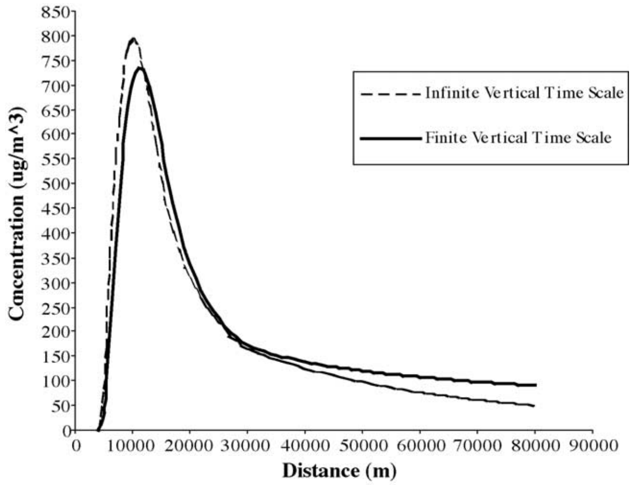

Fig. 2. Effect of finite vertical Lagrangian time scale.

where

$$f_{lz}(x, x') = \left[1 + \frac{0.5(x - x')}{UT_{lz}}\right]^{1/2} \tag{3.54}$$

After Weil et al. [31], T_{lz} is considered as $T_{lz} = T_{ly} = 0.7 z_i/w_*$. This shows good agreement with observed data for the Nanticoke power plant (discussed in the later section).

In Eq. (3.54) the term $f_{lz}(x, x')$ will move the point of maximum concentration further downwind, because the vertical dispersion reduces by incorporating that term. The effect of the finite Lagrangian integral time scale is presented in Fig. 2. In finite T_{lz} case, the concentration is lower for small distances and higher for large distances than those for infinite T_{lz}. This can be attributed to the reduced vertical dispersion initially, causing more plume material to get dispersed at long tails, with the inclusion of finite T_{lz}.

4. Model's performance evaluation

Several field and laboratory experiments have been undertaken to characterize the phenomenon of coastal fumigation. One of the most comprehensive coastal dispersion experiments was conducted at Nanticoke during May 29 to June 16, 1978, designated hereafter as EXP I. The results of this study would be used to carry out performance evaluation of the current model.

This section reviews the experimental program (EXP I) in brief and describes a framework to evaluate the performance of air quality model. Statistical analysis of the current model and its comparison with the two previous studies based on the models of Misra [19] and Luhar and Sawford [12] are also presented.

4.1. Experimental program

EXP I, carried out by the Atmospheric Environment Service (AES) of Environment Canada in cooperation with the Ontario Ministry of the Environment (OME) and Ontario Hydro, was commenced to obtain detailed meteorological measurements of the vertical structure of onshore flows, boundary layer development and surface and airborne pollutant measurements during fumigation conditions.

Nanticoke is situated on the northern shore of Lake Erie. The electric power generating station of Ontario Hydro at Nanticoke has two 198 m stacks separated by 273 m. This coal-fired power plant has a generating capacity of 4000 MW. At design full load (4000 MW) and using coal containing 2.3% sulfur, emission of SO_2 of magnitude of 16 kg/s is expected from these stacks [20]. During the field experiments the SO_2 emission rate remained at about 5 kg/s.

Many systems, including tethersonde, minisonde, acoustic sounder and sonic anemometers, were deployed to measure the height and structure of both the TIBL as a function of inland distance during onshore flow and the stable layer aloft.

A LIDAR unit, operated from a mobile van, was used to measure plume rise, plume bearing and its dispersion characteristics as a function of downwind distance. Three correlation spectrometers (COSPEC) were mounted in three different vehicles. The two COSPEC vehicles also had Sign-X SO_2 monitors to obtain the ground level distribution of SO_2 simultaneously with the overhead SO_2 burden while traversing. Fixed ground level Philips SO_2 monitors and mobile chemistry laboratories augmented these data sets. A helicopter and an aircraft platform were also used to measure SO_2.

During the study period, gradient or lake breeze flows transported the Nanticoke power plant plume inland only on 8 days: 29, 30 May; 1, 4, 6, 12, 15 and 16 June. Two days, June 1 and 6, 1978, were selected for comprehensive presentation as data coverage was considered better than on other days and two noticeably different fumigations existed.

On the 1st June light gradient flow allowed for a lake breeze, which veered with time of day resulting in a systematic clockwise rotation of the fumigation zone. On the 6th June relatively fixed fumigation was reported during steady gradient onshore flow. Further details of EXP I may be found in Portelli [21].

4.2. Model testing and validation methodology

Venkatram [24] described a framework to evaluate air quality model predictions against observations. He proposed the following relationship between observations and predictions from a model:

$$C_o(x_1, x_2) = C_p(x_1) + \varepsilon(x_2) \tag{4.1}$$

where $C_p(x_1)$ represents the predicted values, which are the functions of inputs (x_1) used in model, x_2 denotes unknown variables, which affect the observed concentration C_o and $\varepsilon(x_2)$ is designated as residual, which is due to unknown variables not included in the model. The observation term $C_o(x_1,$

x_2) is made up of a deterministic part, $C_p(x_1)$, as well as a stochastic part, $\varepsilon(x_2)$. In the above equation it is assumed that inputs to model and observed values are error free.

A residual analysis, where magnitude of arithmetic mean is zero or close to zero and magnitude of geometric mean (in case of log transformation) is 1 or close to 1 but the standard deviation is large does not ensure a good performance of the model. On the other hand a residual analysis, where ideal mean value is not achieved but yields a small standard deviation, can perform more effectively. So, in the current study mean absolute error (MAE) and mean relative error (MRE) for residuals are also used as quantitative measures besides the mean and standard deviation. Mean absolute error is reported as:

$$\text{MAE} = \frac{1}{N}\sum_{i=1}^{N}|\varepsilon| \tag{4.2}$$

Mean relative error is defined as:

$$\text{MRE}\,(\%) = \frac{100}{N}\sum_{i=1}^{N}\frac{|\varepsilon|}{C_o} \tag{4.3}$$

where N represents the sample size and ε is given as:

$$\varepsilon = C_o - C_p \tag{4.4}$$

where C_o and C_p represent the observed and predicted concentrations, respectively.

So a model having the low standard deviation of residuals, MAE and MSE should show good performance. Moreover, the condition that ε is independent of input variables x_1, should be fulfilled (Venkatram [24]). From Draper and Smith [5], if ε is not a function of x_1 the plot should look like a band distributed around $\varepsilon = 0$.

Table 1
Input to the model

Day (h)	Downwind distance (km)	Lateral distance (km)	U/w_*	w_* (m/s)	A_0 ($m^{1/2}$)	Brunt–Vaisalla frequency (s^{-1})	Buoyancy flux (m^4/s^3)			Emission rate (Kg/s)
							S1[a]	S2[b]	Average[c]	
1–11	16.4	−1	3.67	1.28	4.95	0.017	564	1053	808.5	6.55
	10	0								
	8	−0.5								
1–12	16	0	3.88	1.29	4.66	0.0144	448	1059	753.5	6.25
	16	1.5								
1–13	15.9	0	3.41	1.38	4.4	0.0176	448	950	699	6.03
	15.4	−0.5								
	15.4	−1								
1–14	15.9	0	4.38	1.28	3.95	0.0192	448	950	699	5.59
	16.1	−0.2								
	16.1	−0.5								
1–15	15.9	0	4.79	1.17	3.56	0.0249	528	949	738.5	5.09
	14.3	0								
	14.3	−0.5								
6–12	14.5	−0.5	5.68	1.32	3.16	0.0188	448	582	515	4.2
6–14	14.2	0	5.05	1.21	2.71	0.0246	448	802	625	5.07
	14.2	−0.5								
	8	−0.5								
6–15	8	0.25	3.97	1.47	5.27	0.013	448	972	710	5.76
	8	−0.25								
	8	0.5								
	8	−0.5								
	14.5	0.5								
	14.5	−0.5								
	14.5	1								
	14.5	−1								
6–16	8	0	4.35	1.47	5.6	0.0092	527	875	701	6.03
	14.5	−0.4								
6–17	14.5	−0.5	5.93	1.17	4.5	0.01	271	500	385.5	5.52
	14.5	−1								
	14	0								

[a] Buoyancy flux from stack 1.
[b] Buoyancy flux from stack 2.
[c] Average buoyancy flux.

Table 2
Predicted and observed concentrations

Day (h)	Downwind distance (km)	Lateral distance (km)	C_p (ppb) Misra's model	C_p (ppb) Luhar's Lagrangian model	C_p (ppb) PDF new	C_o (ppb) observed
1–11	16.4	−1	124	179.4	187	87
	10	0	590	351.4	476	410
	8	−0.5	276	219.1	234	250
1–12	16	0	435	307.6	369	243
	16	1.5	23	100.8	61	243
1–13	15.9	0	437	246.2	389	400
	15.4	−0.5	308	276.03	330	185
	15.4	−1	118	211.42	184	185
1–14	15.9	0	422	311.1	397	400
	16.1	−0.2	335	335	378	165
	16.1	−0.5	237	245	300	165
1–15	15.9	0	382	264.4	399	217
	14.3	0	287	322.4	400	363
	14.3	−0.5	177	167.2	285	363
6–12	14.5	−0.5	189	58.9	134	145
6–14	14.2	0	160	163.64	191.5	114
	14.2	−0.5	92	115.8	118	114
	8	−0.5	31	36	0	36
6–15	8	0.25	436	403	268	355
	8	−0.25	436	403	268	355
	8	0.5	180	217.2	161	355
	8	−0.5	180	217.2	161	355
	14.5	0.5	243	213	251	78
	14.5	−0.5	243	213	251	78
	14.5	1	26.4	164.4	121	78
	14.5	−1	26.4	164.4	121	78
6–16	8	0	696	273.8	221	710
	14.5	−0.4	288	147.8	234	209
6–17	14.5	−0.5	267	210	216	190
	14.5	−1	60	70	51	190
	14	0	488	303	357	400

4.3. Model inputs and results

The parameters used as input to the model include: temperature, mean wind speed, convective velocity w_*, a parameter A_0 to predict the growth of the TIBL, effective Brunt–Vaisala frequency of onshore flow and emission rate. These parameters are obtained from Kerman [9] and Misra and Onlock [20] and are presented in Table 1.

The final plume rise is calculated for each stack and then the mean rise is calculated by assuming the same loading on each stack. Results obtained from the current model, Misra's [19] model, Lagrangian stochastic model from Luhar and Sawford [12] and field observations from Misra and Onlock [20] are presented in Table 2. Comparing different models it is clear that the current model is in better agreement with field observations.

4.4. Statistical analysis and discussion

For the performance evaluation of a model the inputs to a model and observed values should be free of error. It is evident from Misra and Onlock [20] that due to an accuracy of $\pm 5^\circ$ in the measurement of wind direction, the crosswind position of monitors was determined within an accuracy of 500–1500 m. Also, source emission rates were not measured during the field experiments, rather they were determined from a mass balance analysis. However, during the current analysis all the observations are considered as free of error except the reading observed at 16:00 h on the 6th June. The magnitude of 710 ppb had not been observed at any other time or day, even though at 15:00 and 16:00 h on the 6th June, the lateral plume spreads and convective velocity was approximately the same and emission rate was also not (considerably) different.

Instead of running the model for average input values for some specific hours as done by Luhar and Sawford [12], here the model is run separately for each hour. The model is very time efficient and running time was less then 5 s (Pentium Pro III, 550 MHz processor). From Table 1 the stability index of U/w_* remains below 6, this shows the strong convection regime during experiments.

The probability plot of residuals for the PDF model is plotted and checked for normality without any transformation.

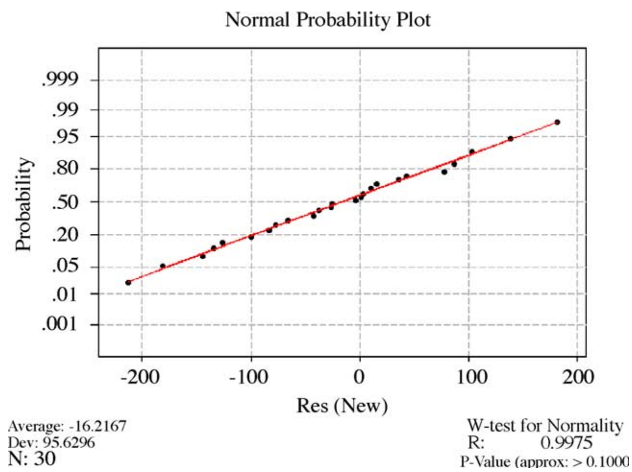

Fig. 3. Normal probability plot for residuals.

From Fig. 3 it is evident that the residuals pass the normality test. The other quantitative measures discussed above are reported in Table 3.

The standard deviation of residuals (S.D.) and mean standard error (MAE) are minimum for the results obtained from the present model. To check for the constant variance of residuals, plots are drawn between residuals and predicted values in Fig. 4a–c.

It is evident from the residual plot, for the present model the residuals are uniformly distributed about zero line. The dispersion of residuals about zero residual line is minimum for the present model. Moreover, the residual plot shows reasonable scatter for present model, without any funnel shape, confirming the constant variance.

Fig. 5a–d shows residual plots against the input parameters for the present model. The distributions of residuals are in bands showing that residuals are independent of model inputs.

Table 3
Quantitative measures of coastal dispersion model performance

Model	Summary measures			
	Mean	S.D.	MAE	MRE (%)
Misra's model	−23	117.8	100.3	55
Stochastic model [12]	5.6	99.4	84.43	49.5
Present model	−16.2	95.6	76.35	46.4

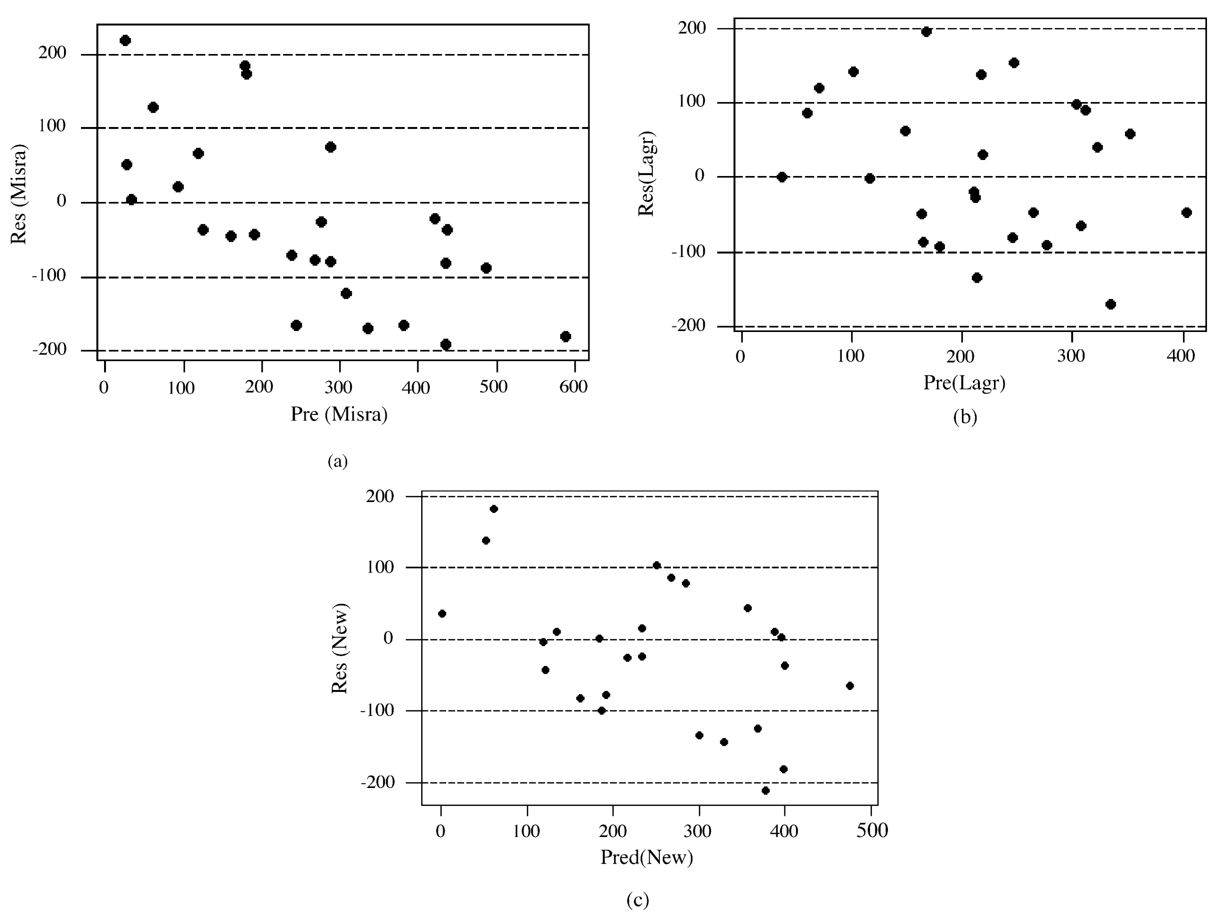

Fig. 4. Plot of residuals (ppb) against predicted concentration values (ppb): (a) Misra's model; (b) Lagrangian model; and (c) Present model.

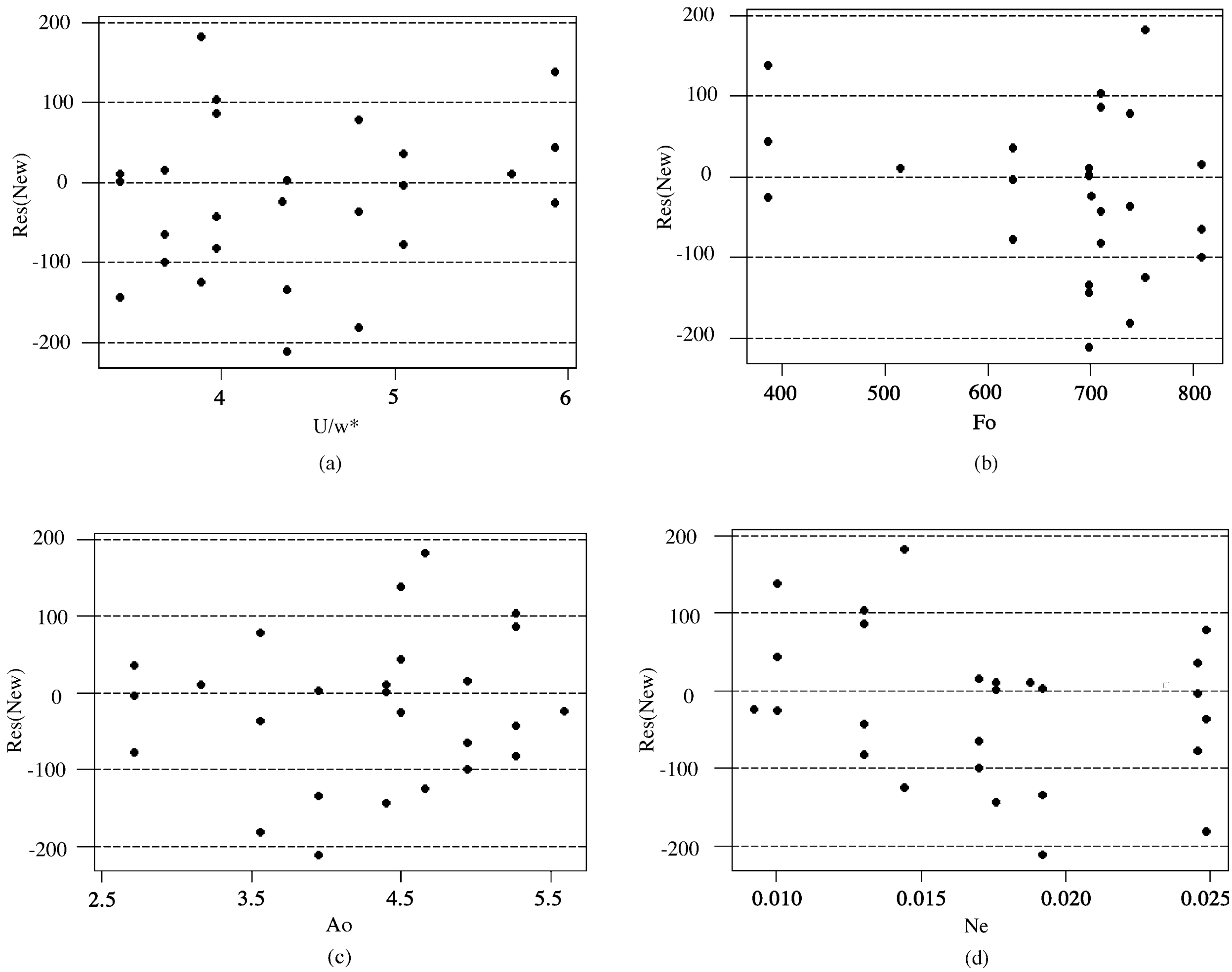

Fig. 5. Plot of residuals (ppb) against model inputs for the new model: (a) residuals against ratio of mean wind speed to convective velocity; (b) residuals against buoyancy flux; (c) residuals against A_0; and (d) residuals against Brunt–Vaisala frequency (N_e).

5. Conclusions

The proposed fumigation PDF model is an approach that includes state-of-the-art knowledge of the TIBL turbulence and dispersion (analogous to CBL) in a simple but effective framework. It is very time efficient and requires few seconds for computation. We demonstrated that assumption of Weil and Brower's [27] convective limit works fair-to-good for the TIBL in the case of fumigation. The proposed model considers the condition of stable onshore flow and uses the slab model to determine the height of the TIBL. The model is restricted to stable onshore flows and strong convective conditions. Characterizing in terms of stability index of U/w_*, the model is applicable in the range of $1.2 < U/w_* < 6$.

In contrast with the Misra's [19] model, the current model relaxes the instantaneous and uniform mixing assumptions in the vertical direction within the TIBL by considering the skewed bi-Gaussian vertical velocity PDF. In comparison with the Luhar and Sawford's [12] Lagrangian stochastic model, the present model is very time efficient and appropriate for operational and routine calculations.

After the inclusion of vertical finite Lagrangian integral time scale T_{lz}, we found that it reduced the vertical dispersion and moved the point of maximum concentration downwind. A key assumption was $T_{lz} = T_{ly}$. As initially, vertical dispersion is reduced and therefore at large downwind distances more pollutant is available to disperse. Due to this we obtained higher concentrations at large distances for finite Lagrangian time scale than infinite Lagrangian time scale. This fact requires further experimental validation involving concentration measurements at large distances.

During the performance analysis of the model, normality test of residuals confirmed their normal distribution without any transformation. Residuals also showed reasonable scatter without funnel shape when plotted against predicted values of the model. Further, the analysis provided the evidence that they were independent of the input variables.

Both the mean absolute error and mean relative error are used as quantitative measures of the coastal dispersion model performance, besides the mean and standard deviation of the residuals. The error analysis proves that the model has minimum error relative to the observed values.

References

[1] J.H. Baerentsen, R. Berkowicz, Monte Carlo simulation of plume dispersion in the convective boundary layer, Atmos. Environ. 18 (1984) 701–712.

[2] G.A. Briggs, Plume rise and buoyancy effects, in: D. Randerson (Ed.), Atmospheric Science and Power Production, US Department Of Energy, 1984, pp. 327–366, NTIS-DE84005177.

[3] J.W. Deardorff, G.E. Willis, Ground level concentrations due to fumigation into an entraining mixing layer, Atmos. Environ. 16 (1982) 1159–1170.

[4] R.R. Draxler, Determination of atmospheric diffusion parameters, Atmos. Environ. 10 (1976) 99–105.

[5] R.N. Draper, H. Smith, Applied Regression Analysis, second ed., John Wiley, NY, 1981.

[6] S. Du, J.D. Wilson, E. Yee, Probability density functions for velocity in the CBL, and implied trajectory models, Atmos. Environ. 28 (1994) 1211–1217.

[7] J.R. Garratt, The Atmospheric Boundary Layer, Cambridge University Press, Cambridge, 1992, pp. 186–189.

[8] B.B. Hicks, Behavior of turbulent statistics in the CBL, J. Climate and Applied Meteorology 24 (1985) 607–614.

[9] B.R. Kerman, A similarity model of shoreline fumigation, Atmos. Environ. 16 (1982) 467–477.

[10] R.G. Lamb, Diffusion in the convective boundary layer, in: F.T.M. Nieuwstadat, D.H. Van (Eds.), Atmospheric Turbulence and Air Pollution Modeling, Reidel Publishing Co., Dordrecht, The Netherlands, 1982, pp. 159–229.

[11] K.Z. Li, A.G. Briggs, Simple PDF models for convective driven vertical diffusion, Atmos. Environ. 22 (1988) 55–74.

[12] A.K. Luhar, B.L. Sawford, Lagrangian stochastic modeling of the coastal fumigation phenomenon, J. Appl. Meteorol. 34 (1995) 2259–2277.

[13] A.K. Luhar, B.L. Sawford, An examination of existing shoreline fumigation models and formulation of an improved model, Atmos. Environ. 30 (1996) 609–620.

[14] A.K. Luhar, An analytical slab model for the growth of the coastal thermal internal boundary layer under near-neutral onshore flow conditions, Boundary-Layer Meteorol. 88 (1998) 103–120.

[15] A.K. Luhar, The influence of vertical wind direction shear on dispersion in the convective boundary layer, and its incorporation in coastal fumigation models, Boundary-Layer Meteorol. 102 (2002) 1–38.

[16] A.K. Luhar, S.A. Young, Dispersion moments of fumigating plumes-LIDAR estimates and PDF model simulations, Boundary-Layer Meteorol. 104 (2002) 411–444.

[17] W.A. Lyons, H.S. Cole, Fumigation and plume trapping on the shores of lake Michigan during stable onshore flow, J. Appl. Meteorol. 12 (1973) 494–510.

[18] P.J. Mason, Large eddy simulation of dispersion in convective boundary layers with wind shear, Atmos. Environ. 26A (1992) 1561–1571.

[19] P.K. Misra, Dispersion from tall stacks into a shoreline environment, Atmos. Environ. 14 (1980) 397–400.

[20] P.K. Misra, S. Onlock, Modelling continuous fumigation of Nanticoke generating station plume, Atmos. Environ. 16 (1982) 479–489.

[21] R.V. Portelli, The Nanticoke shoreline diffusion experiment, June, 1978-I: experimental design and program overview, Atmos. Environ. 16 (1982) 413–421.

[22] R.B. Stull, An Introduction to Boundary Layer Meteorology, Kluwer Academic Publishers, Dordrecht, The Netherlands, 1988, p. 450.

[23] A. Venkatram, A model of internal boundary layer development, Boundary-Layer Meteorol. 11 (1977) 419–437.

[24] A. Venkatram, A framework for evaluating air quality models, Boundary-Layer Meteorol. 24 (1982) 371–385.

[25] A. Venkatram, Topics in applied dispersion modeling, in: A. Venkatram, J.C. Wyngaard (Eds.), Lectures on Air Pollution Modeling, American Metrological Society, Boston, MA, 1988, pp. 267–324.

[26] D.H. Van, R. Steenkist, E.T.M. Nieustadt, Revised estimates for continuous shoreline fumigation, J. Appl. Meteorol. 18 (1979) 133–137.

[27] J.C. Weil, P.R. Brower, Estimating convective boundary layer parameters for diffusion applications, in: Maryland Power Plant Siting Program Rep. PPSP-MP-48, Department of Natural Resources, Annapolis, MD, 1984, 37 pp.

[28] J.C. Weil, A.L. Corio, Dispersion formulations based on convective scaling, in: Maryland Power Plant Siting Program Rep. PPSP-MP-60, Department of Natural Resources, Annapolis, MD, 1985, 39 pp.

[29] J.C. Weil, Dispersion in the convective boundary layer, in: A. Venkatram, J.C. Wyngaard (Eds.), Lectures on Air Pollution Modelling, American Meteorological Society, Boston, MA, 1988, pp. 167–227.

[30] J.C. Weil, A diagnosis of the asymmetry in top-down and bottom-up diffusion using a Lagrangian stochastic model, J. Atmos. Sci. 47 (1990) 501–515.

[31] J.C. Weil, L.A. Corio, P.R. Brower, A PDF dispersion model for buoyant plumes in the convective boundary layer, J. Appl. Meteorol. 36 (1997) 982–1003.

[32] J.C. Wyngaard, Structure of the PBL, in: A. Venkatram, J.C. Wyngaard (Eds.), Lectures on Air Pollution Modelling, American Meteorological Society, Boston, MA, 1988, pp. 9–61.